Journal of Biomolecular Structure and Dynamics

http://www.jbsdonline.com

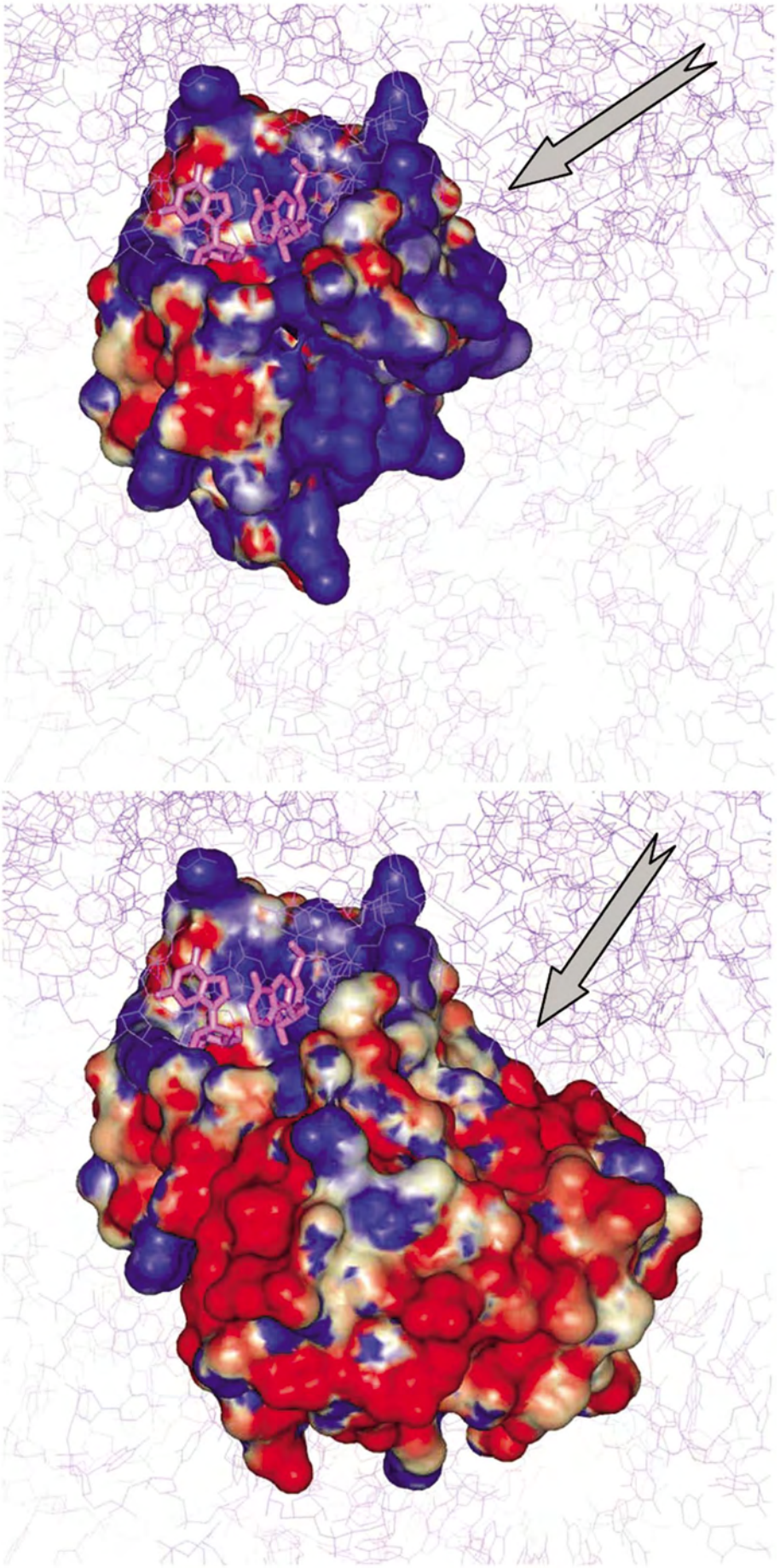

Volume 20,
Issue Number 5
April 2003
ISSN 0739-1102

A Bimonthly Publication
of Adenine Press

Journal of Biomolecular Structure & Dynamics, ISSN 0739-1102
Volume 20, Issue Number 5, (2003)

Prediction of the Structure of the Complex Between the 30S Ribosomal Subunit and Colicin E3 via Weighted-Geometric Docking

http://www.jbsdonline.com

Efrat Ben-Zeev[1,#]
Raz Zarivach[2,#]
Menachem Shoham[3]
Ada Yonath[2,4]
Miriam Eisenstein[5,*]

[1]Weizmann Institute of Science
Department of Biological Chemistry
Rehovot, 76100 Israel.
[2]Weizmann Institute of Science
Department of Structural Biology
Rehovot, 76100 Israel.
[3]Case Western Reserve University
School of Medicine
Department of Biochemistry
Cleveland, OH 44106-4935, USA.
[4]Max-Planck-Research Unit for
Ribosomal Structure
Notkestrasse 85
22603 Hamburg, Germany.
[5]Weizmann Institute of Science
Department of Chemical Services
Rehovot, 76100 Israel

#These authors contributed equally.

*Phone: 972-8-9343031
Fax: 972-8-9344136
Email: miriam.eisenstein@weizmann.ac.il

Abstract

Colicin E3 kills *Escherichia coli* cells by ribonucleolytic cleavage in the 16S rRNA. The cleavage occurs at the ribosomal decoding A-site between nucleotides A1493 and G1494. The breaking of this single phosphodiester bond results in a complete termination of protein biosynthesis leading to cell death. A model structure of the complex of the ribosomal subunit 30S and colicin E3 was constructed by means of a new weighted-geometric docking algorithm, in which interactions involving specified parts of the molecular surface can be upweighted, allowing incorporation of experimental data in the docking search. Our model, together with available experimental data, predicts the role of the catalytic residues of colicin E3. In addition, it suggests that bound acidic immunity protein inhibits the enzymatic activity of colicin E3 by electrostatic repulsion of the negatively charged substrate.

Introduction

Colicins are plasmid-encoded exotoxins secreted from *Escherichia coli* (*E.coli*) to kill related bacterial strains. Colicins kill *E.coli* cells in three steps: receptor binding, translocation and cytotoxicity. These activities are localized on three separate domains. The central (R) domain is responsible for the binding of the colicin to its receptor, whereas the translocation across the cytoplasmic membrane involves the N-terminal (T) domain. The C-terminal (C) domain is responsible for the cytotoxicity of colicins, which in E colicins is caused either by cytoplasmic membrane depolarization (colicin E1), by non-specific endonuclease activity that degrades DNA (colicins E2, E7, E8 and E9) or by ribonuclease activity that cleaves specifically transfer RNAs (colicin E5) or ribosomal RNA (colicins E3, E4 and E6) (1).

Colicin E3 (colE3) specifically cleaves a single phosphodiester bond of the *E.coli* 16S ribosomal RNA, which contains more than 1500 nucleotides (2). The cleavage site, between A1493 and G1494 (*E.coli* numbering system), is near the interface between the small and large ribosomal subunits, at a critical position for the interactions of the A-site tRNA and the mRNA with the ribosome (3). The cleavage by colE3 results in a complete inactivation of the ribosome leading to the death of the attacked cell. One of the nucleotides at the cleavage site, A1493 (together with A1492 and G530) is actively involved in selecting and binding of cognate tRNA (4). In addition, it was found that the initiation factor 1 (IF1) binds to the two nucleotides of 16S rRNA immediately preceding the colE3 cleavage site (5). Hence, it is likely that the colE3 cleavage cripples the ribosome by blocking the initiation of protein biosynthesis.

The resistance of the producing organism towards colE3 is due to the presence of an immunity protein (IP), which forms a tight 1:1 complex with colE3 (6). Free IP is produced in large excess by the cell to protect it from the toxicity of either

endogenous or exogenous colE3, and when isolated under mild conditions, colE3 is always found in the complexed form with IP.

The structural details of the interaction between the RNase domain of colE3 and the 30S ribosomal subunit are yet to be revealed experimentally. Also, the mechanism of the inhibition of colE3 activity by IP is not known, as it does not block the active site of colE3 (7). In this study we present an *in silico* model of the transient complex between the RNase domain of colE3 (8) and the 30S ribosomal subunit (5, 9, 10). Notably, the only available experimental structure of the 30S ribosomal subunit is from *Thermus thermophilus* (*T.t.*). The sequence of this subunit is highly conserved in the vicinity of the cleavage site, and the structure in this area is expected to be similar to that of the 30S subunit from *E.coli* (11). Moreover, an inactive mutant of colE3 binds to *T.t.* (12). Therefore, we assume that docking colE3 to the 30S ribosomal subunit from *T.t.* provides a good model of its interactions with the 30S subunit from *E.coli*.

The predicted model structure of the complex between the 30S ribosomal subunit and colE3 suggests a plausible catalytic mechanism for the rRNA cleavage, in line with the results of site-specific mutagenesis of colE3 active site residues (7). It also suggests that the inhibitory action of bound IP is due to electrostatic repulsion of the substrate and not to steric hindrance.

Materials and Methods

The model structure of the complex between ribosomal 30S subunit and colE3 was obtained by protein-protein docking. We used the program MolFit (13), which projects each molecule onto a 3D grid and calculates the correlation function between the two grid-representations. MolFit treats the molecules as rigid bodies and distinguishes between their surface and interior. It performs a full rotation/translation scan calculating for each relative position a correlation value (score), which estimates the degree of geometric surface complementarity. In this study we designed and tested a modified version of MolFit, in which contacts involving specified residues are up-weighted.

In regular geometric docking the grid points on the molecular surfaces have the value 1, and the potential contribution of all these points to the complementarity score is equal. In the weighted-geometric docking algorithm we change the value of grid points derived from specified residues of molecule **a** (the 30S ribosomal subunit in this study) from 1 to $1 + it$, where t is a positive adjustable weight parameter and i is the square root of –1. The grid points of molecule **b** (colE3 in this study) are given the value $1 - i$. The parameter t is 0 in regular (un-weighted) geometric docking and it remains 0 for most of the molecular surface in the weighted-geometric docking. This parameter is made non-zero only for grid points derived from a few specified residues. When molecules **a** and **b** are in contact, i.e. their surfaces overlap, the contribution to the correlation value from regular residues is: $1 - i$. The contribution from the specified residues is: $(1 + t) + i(t - 1)$. As only the real part of the correlation matrix is considered, the contribution of regular residues to the correlation score remains 1 whereas the contribution of the special residues is larger than 1 and it depends linearly on t.

The structure of the ribonuclease domain of colE3 with the highest resolution (8) was used in docking (PDB entry 1e44). This structure is of a complex between the ribonuclease (C) domain of colE3 and IP. The IP was omitted and so were the N-terminal residues 455-464 of the C domain of colE3, which interact with IP but not with the rest of colE3. This structure was docked to 3 structures of the 30S subunit: The native *T.t.* 30S (14) (PDB code 1i94), the *T.t.* 30S subunit from the complex 30S:paromomycin (10) (PDB code 1fjg) and the *T.t.* 30S subunit from the complex 30S:IF1 (5) (PDB code 1hr0). All the water molecules were omitted as well as the Mg ions, the tungsten

cluster and the terminal regions of the proteins that bind the tungsten cluster (residues S2: 2-38, 226-250, S18: 7-21) in native 30S. Correspondingly, we omitted from the 30S:paromomycin and 30S:IF1 structures a fragment of messenger RNA, Mg and Zn ions, and the paromomycin and IF1 molecules.

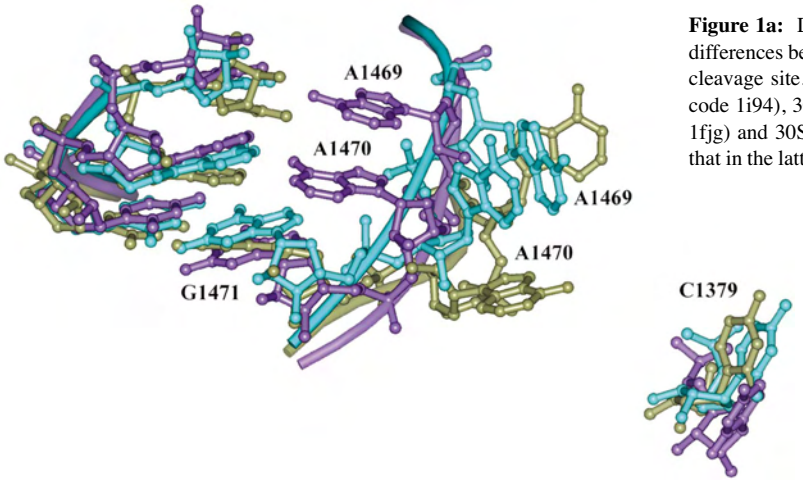

Figure 1a: Docking of colE3 to the 30S ribosomal subunit. (a) Structural differences between three 30S ribosomal subunits in the vicinity of the colE3 cleavage site. The native 30S ribosomal subunit is shown in purple (PDB code 1i94), 30S from the 30S:paromomycin complex is in cyan (PDB code 1fjg) and 30S from the 30S:IF1 complex in khaki (PDB code 1hr0). Note that in the latter two structures nucleotides A1469 and A1470 are flipped out.

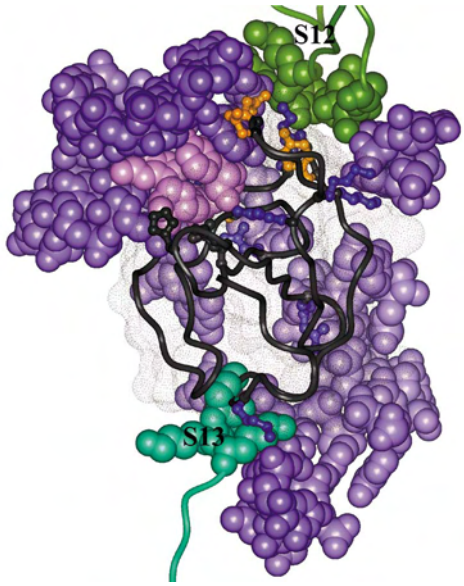

Figure 1b: Docking of colE3 to the 30S ribosomal subunit. (b) Docking model of colE3 to native 30S (model N2). The 16S rRNA is colored purple except for the cleavage site nucleotides, which are emphasized in pink. S12 and S13 are colored in different shades of green (S13 was taken from the complex 30S:paromomycin and superposed on native 30S). The colE3 molecule is depicted as black dot surface and ribbon with the catalytic triad residues shown in ball and stick. Other colE3 residues, which interact with the 30S ribosomal subunit (see text) are shown in blue (lysine and arginine side chains) or orange (asparagine, glutamine, serine and tyrosine side chains). The figure was generated using the Accelrys package (Accelrys Inc., San-Diego, CA).

Each molecule was projected onto a 250×250×250 grid with a grid interval of 1.28-1.30Å, depending on the specific structure of the 30S subunit. The angular interval in each scan was 12°, resulting in 8760 relative orientations (15) and for each orientation we kept only one best match. The same intervals were used in the weighted-geometric scans, where an extra weight, t=1, was given to grid points derived from nucleotides 1470 and 1471. These *T.t*. nucleotides correspond to residues 1493 and 1494 in *E.coli*. It is important to note that despite the large size of the 30S ribosomal subunit the resolution of our procedure is not compromised. By enlarging the grid we obtain digitized representations of the docked molecules, which are of similar resolution to the representations commonly used for docking of globular proteins (16).

The 8760 solutions from each rotation-translation scan were sorted by their complementarity scores and an extreme value distribution function (17) was fitted to the observed distribution of scores, providing a measure of the uniqueness of the different docking solutions (16).

Results and Discussion

Docking of colE3 onto the 30S Ribosomal Subunit

Several crystallographic structures of the 30S ribosomal subunit are available in the Protein Data Bank (18) (PDB), all from *T.t*. Therefore, in the following sections we use the nucleotide-numbering scheme of *T.t*. and add the corresponding *E.coli* num-

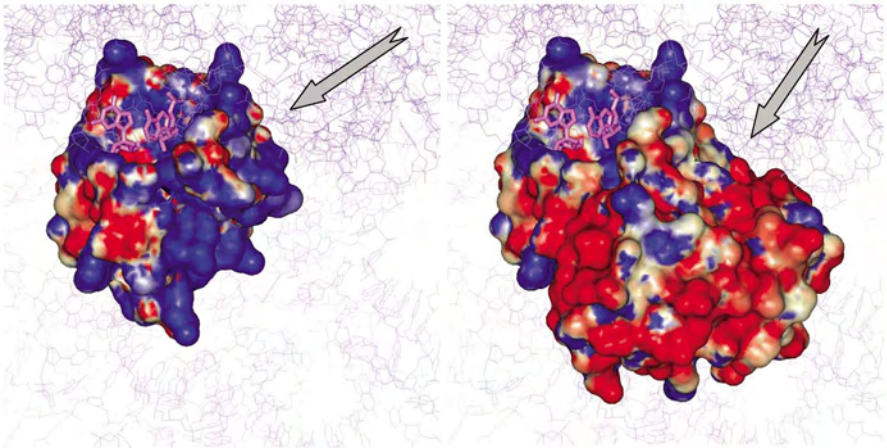

Figure 1c: Docking of colE3 to the 30S ribosomal subunit. (c) Docking model of colE3 to native 30S (model N2) showing the electrostatic potential. The 30S subunit is colored purple except for the cleavage site nucleotides, which are emphasized in pink. The solvent accessible surface of colE3 (left panel) is colored according to the electrostatic potential (red for negative; blue for positive), calculated with the program Delphi (25), as implemented in the Accelrys package. Note the basic character of the surface that interacts with the 30S ribosomal subunit (where the arrow points). On the right panel the complex colE3:IP is shown after superposition on the colE3 molecule in model N2. The electrostatic potential was calculated for the whole complex. Note the acidic character of the surface that now faces the 16S rRNA, away from the active site. This suggests a mechanism for the inhibitory action of IP.

bering in parenthesis. Nucleotides A1470 and G1471 (corresponding to A1493 and G1494 in *E.coli*) have different conformations in each of the three crystallographic structures of the 30S ribosomal subunit (see Figure 1a). Thus, in native 30S these nucleotides point inwards, G1471 forms a Watson-Crick pair with C1389 (C1407 in *E.coli*) and A1470 interacts with A1390. The sugar-phosphate backbone of both nucleotides is exposed. In the 30S:IF1 complex the Watson-Crick base pair G1471-C1389 is conserved but a change in the propeller twist for this base pair occurs compared to native 30S. In contrast, A1470 and A1469 flip out, exposing both purine rings. A similar flip occurs in the 30S:paromomycin complex. However, in the latter structure the nucleotides adopt a different conformation, in which the exposed purine rings are stacked. Additional structural differences occur in the vicinity of the cleavage site. The most prominent of these is the different conformation of C1379 (C1397 in *E.coli*). ColE3 was docked to each of the three 30S structures, anticipating that comparison of the results will provide insight regarding the conformation of nucleotides A1470 and G1471 in the 30S:colE3 complex.

In the weighted-geometric docking the portion of the surface of 30S belonging to nucleotides A1470 and G1471 was given extra weight. Hence, the available biochemical information on the cleavage site in the 16S rRNA was used in the docking scan, emphasizing solutions in which colE3 resides near these residues. In contrast, *none of the colE3 residues was given extra weight*, although we knew where the active site of this protein resides (7). The orientation of colE3 relative to the 30S subunit was therefore, unconstrained. The biochemical information about the active site residues of colE3 was used only to analyze the predicted models (see below).

The top ranking solutions from each docking scan, i.e. those with complementarity scores within the top 5 standard deviations (5σ), were viewed and analyzed. In the weighted geometric scan to native 30S the mean score was 444.5 (arbitrary score units) and we analyzed 41 solutions with scores ranging from 860 to 663 (σ for this scan was 39.4). In the top ranking solution colE3 is located near the rRNA cleavage site. However, its active site residues face the solvent and therefore, this solution was discarded. In the second ranking solution (model N2) the active site of colE3 faces the 16S rRNA cleavage site and the active site residues are within 3.3Å from nucleotides A1470 and G1471. The score of this model (804) is 1.4σ below that of the top solution, probably because of the clash between Arg545 of colE3 and the phosphate group of nucleotide G1471, which can be relieved by choosing an alternative rotamer for Arg545. ColE3 in model N2 fits snugly into the 30S subunit and forms many contacts, resulting in a high complementarity score despite the clash. The score of the third solution in this scan is much lower (745), 2.9σ below the top. Therefore, model N2, which is in accord with biochemical data, is considered a plausible model-structure for the transient binding of colE3 to the 30S subunit. Notably, this is a highly unique solution, scoring 9.1σ above the mean score. In the regular geometric scan to native 30S (without weighting), the same solution is ranked 136 with a score of 575 units (3.8σ above mean score). The large increase in the score for model N2 in the weighted geometric scan (229 units more than in the geometric score), reflects the extent of the interactions of nucleotides A1470 and G1471 with colE3.

When colE3 is docked to the 30S subunit taken from the complex 30S:paromomycin, a solution similar to model N2 is ranked third with a score of 733 units (1.1σ from the top). In this solution (model P3) the distances between the active site residues of colE3 and nucleotides A1470 and G1471 are slightly larger than in model N2, probably because of the different conformation of the nucleotides. A model similar to P3 is found in the weighted-geometric scan of colE3 to the 30S subunit from the 30S:IF1 complex, in which yet another conformation of the bases A1470 and G1471 is observed. This model is ranked 4.4σ below the top solution.

Analysis of the weighted-geometric docking solutions in the top 5σ range of scores identifies a cluster of three similar solutions in the weighted-geometric docking to

native 30S and a cluster of five similar solutions is found in the docking to 30S from the 30S:paromomycin complex. Inspection of the latter cluster indicates that in all five models the residues in the putative active site of colE3 are approximately in the same position with respect to A1470 and G1471, while the rest of the molecule pivots around this point.

The Predicted Structure for the Complex 30S:colE3

The high complementarity score and the exceptional uniqueness of solution N2, and in particular the positioning of residues implicated in the RNase activity of colE3 next to nucleotides A1470 and G1471 in the 30S subunit, render N2 a likely model of the structure of the complex 30S:colE3. Examination of other parameters, such as the electrostatic interactions between colE3 and the 16S rRNA backbone, further supports this solution (see below). These interactions are not included in the geometric or weighted-geometric docking process and can, therefore, be used to verify the model.

The 30S:colE3 model is in accordance with other biochemical and structural data. For example, colE3 was found to interact with intact 70S ribosomes and to inactivate them both *in vivo* and *in vitro* (19, 20). Superposition of our proposed 30S:colE3 structure onto the70S ribosomal subunits (3) (PDB code 1gix) indicates that colE3 makes no contacts with the large (50S) ribosomal subunit. Also, superposition of the model on the experimental 30S:paromomycin complex, which includes mRNA, suggests that mRNA and colE3 binding to the 30S subunit are mutually exclusive. Similarly, binding of tRNA at the A-site and colE3 are mutually exclusive. These predictions are in agreement with the experimental results that binding of mRNA as well as tRNA protects ribosomes from colE3 attack (21, 22). In contrast, the ribosomal P-site, consisting of nucleotides 1210, 1319-1320, 1382 and 1475 in 16S (1229, 1338-1339, 1400 and 1498 in *E.coli* numbering) and the carboxy-terminal ends of proteins S13 (residues 116-120) and S9 (3) is free, according to our model, to bind tRNA in the presence of colE3.

Figure 1b depicts the predicted structure of the complex between native 30S and colE3, in which the active site of colE3 wraps around the conserved upper part of helix H44. The accuracy of our model is limited by the rigid body docking approximation, the grid interval, and to some extent, by the resolution of the input structures. Therefore, our model can only be an approximation to the real structure and in the analysis below we consider intermolecular distances up to 5.0Å. In addition, our previous experience suggests that when clusters of solutions are formed, the solution with the highest score is not necessarily the most accurate; hence in the analysis below we consider the intermolecular distances in all the solutions in the clusters.

In addition to the interactions of the catalytic triad residues with the cleavage site nucleotides (see below), the recognition between 30S and colE3 is facilitated by interaction of several colE3 loops with different 16S rRNA domains, with protein S12 and possibly with protein S13. Loops 471-480 and 500-505 of colE3 are within interaction distance with the 30S head (helices H34, H30, H31 of the 16S rRNA), mostly via electrostatic interactions. For example, Lys474, Lys502 and Arg504 interact with the rRNA backbone O1P atoms of nucleotides U932, A941 and G1179, respectively (U955, A964 and G1198 in *E.coli*). Loops 483-495 and 548-551 of colE3 bridge between H18 in the shoulder of 30S and the penultimate helix H44, which interacts with the 50S subunit in the assembled ribosome. Several ionic interactions are formed with the 16S rRNA phosphates (for example Lys485 interacts with C501, Lys494 with C502 and Lys549 with A1469; the corresponding *E.coli* residues are C518, C519 and A1492), as well as polar interactions with the ribose moieties (for example Arg495 with A1470, Asn490 with C1391 and Tyr550 with A1469; the corresponding *E.coli* residues are A1493, C1409 and A1492). In addition, Gln489 interacts with the minor groove of A1469. Loop 483-495 also makes several polar interactions with protein S12. Loop 520-525 of colE3 interacts with H28 in the neck region of 30S, forming an

ionic interaction between Arg520 and the phosphate of G1383 (G1401 in *E.coli*) and polar interactions between Gln525 and the phosphate of C1384 and between Ser522 and the pyrimidine ring of the flipped-out nucleotide C1379 (C1402 and C1397 in *E.coli*). Loop 540-545 approaches the major groove and Lys544 interacts with N7 and O6 of G1387 (G1405 in *E.coli*). Polar interactions between residues 120-123 of S13 and colE3 are observed only in model P3, just beyond the tRNA P-site.

Mutations of the catalytic triad residues (Asp510, His513 and Glu517) in colE3 to alanine abolish its activity and mutation of Arg545 diminishes it (7). In our model these residues are at interaction distance to the cleavage site between nucleotides A1470 and G1471. In model N2 and the other models in the cluster, another histidine, His526, is close to the cleavage site nucleotides. However, in model P3 His513 is positioned next to the O2' atom of the ribose ring of G1471, whereas His526 is 11Å away (similar distances, ranging from 8.6Å to 12.8Å, are observed in other models in the cluster that includes model P3). Hence, our docking results suggest that His526 may be involved in the catalytic activity of colE3, but this result is inconclusive. Based on our prediction His526 was mutated to alanine. It was found that this mutation does not affect the activity of colE3 (12), leaving His513 as the only essential active site histidine.

The predicted model together with the experimental results can be used to propose a mechanism for the specific cleavage of 16S rRNA by colE3 (12), which is similar to the mechanism proposed for ribonuclease T1 by Takahashi and Moore (23). The cleavage occurs in two steps and involves residues Asp510, His513 and Glu517. In the first step a proton is abstracted from the ribose O2´ hydroxyl of nucleotide A1470 by Glu517, leading to the formation of a negatively charged cyclic 2´-3´ phosphate intermediate. The role of Arg545 is to stabilize this intermediate via electrostatic interactions. Notably, Arg545 clashes with nucleotide G1471 in our docking model but when another rotamer is chosen the clash is relieved and good electrostatic interactions are formed with the rRNA backbone. The second step in the enzymatic cleavage by colE3 the hydrolysis of the 2´-3´ cyclic phosphate intermediate. Glu517 acts as a general acid, donating its proton to the O2´ oxygen atom, while Asp510 stabilizes the protonated state of His513. This enables His513 to donate a proton to the leaving 5´-OH RNA fragment upon cleavage.

Inhibition of the RNase Activity of colE3 by IP

The RNase site of colE3 in the complex colE3:IP is exposed; hence the inhibition of the RNase activity by IP is not achieved by blocking the active site. Another possible mechanism of inhibition would be prevention of access to the substrate. Superposition of the structure of the colE3:IP complex onto the colE3 molecule in our model N2 reveals that there are no steric clashes between IP and the 30S ribosomal subunit (see Figure 1c). However, we find many negatively charged residues of IP pointing in the direction of the 30S rRNA backbone, resulting in strong electrostatic repulsion. For example, Asp67 and Asp70 of IP point toward the phosphate groups of C1191 and C1190 (C1209 and C1210 in *E.coli*). Moreover, several stabilizing interactions between positive residues of colE3, such as Lys485 and Lys494, and the 16S rRNA backbone, are weakened by interactions with the negative residues Glu14 and Asp49 of IP. This is reflected in the change in the electrostatic potential when colE3 is bound to IP, indicated by the arrows is Figure 1c. Hence, the inhibition of RNase activity by IP can be attributed to the strong electrostatic repulsion of the 30S subunit. Notably, the immunity protein is highly acidic, with a PI of 4.0 (24). ColE3 must therefore, be separated from IP in order to act upon the 30S subunit.

Conclusions

We present in this study a weighted-geometric docking algorithm, in which interactions involving specified residues are up-weighted, and apply it to predict the

mode of interaction of colE3 with the 30S ribosomal subunit. The model was used to propose mutation experiments, and made it possible to propose a mechanism for the enzymatic cleavage of the 16S rRNA by colE3. The model also provided an explanation for the inhibition of the RNase activity by the immunity protein.

The proposed model-structure is formed also in regular geometric docking, but the weighted-geometric docking procedure emphasizes it over other structures by elevating the complementarity score. Similar high-scoring docking solutions are found in the weighted-geometric docking to native 30S and to 30S subunits taken from the complexes with paromomycine or IF1, although, in the last case the solution is significantly less unique. Interestingly, in the docking to native 30S, the colE3 molecule fits snugly to the 30S subunit, whereas in the docking to 30S from 30S:paromomycin the active site of colE3 is slightly shifted away from the rRNA cleavage site. In the latter case a cluster of high-scoring solutions is formed, in which the whole colE3 molecule pivots about its active site. Based on these results we propose that the conformation of nucleotides A1470 and G1471 in native 30S is more adequate for interaction with colE3 than the conformation of the corresponding nucleotides in the 30S subunits from the complexes with paromomycin or IF1.

Acknowledgements

This study was funded by the Kimmelman Center for Macromolecular Assembly, the US National Science Foundation grant MCB97-28420 of (M.S.) and the US National Institute of Health grant GM34360 (A.Y.). A.Y. holds the Martin S. Kimmel Professorial Chair at the Weizmann Institute of Science.

References and Footnotes

1. R. James, C. Kleanthous, and G. R. Moore, *Microbiology 142*, 1569 (1996).
2. C. M. Bowman, J. E. Dahlberg, T. Ikemura, J. Konisky, and M. Nomura, *Proc. Natl. Acad. Sci. USA 68*, 964 (1971).
3. M. M. Yusupov, G. Z. Yusupova, A. Baucom, K. Lieberman, T. N. Earnest, J. H. Cate, and H. F. Noller, *Science 292*, 883 (2001).
4. J. M. Ogle, D. E. Brodersen, W. M. Clemons, Jr., M. J. Tarry, A. P. Carter, and V. Ramakrishnan, *Science 292*, 897 (2001).
5. A. P. Carter, W. M. Clemons, Jr., D. E. Brodersen, R. J. Morgan-Warren, T. Hartsch, B. T. Wimberly, and V. Ramakrishnan, *Science 291*, 498 (2001).
6. K. Jakes, N. D. Zinder, and T. Boon, *J. Biol. Chem. 249*, 438 (1974).
7. S. Soelaiman, K. Jakes, N. Wu, C. Li, and M. Shoham, *Mol. Cell 8*, 1053 (2001).
8. S. Carr, D. Walker, R. James, C. Kleanthous, and A. M. Hemmings, *Structure Fold Des. 8*, 949 (2000).
9. F. Schluenzen, A. Tocilj, R. Zarivach, J. Harms, M. Gluehmann, D. Janell, A. Bashan, H. Bartels, I. Agmon, F. Franceschi, and A. Yonath, *Cell 102*, 615 (2000).
10. A. P. Carter, W. M. Clemons, D. E. Brodersen, R. J. Morgan-Warren, B. T. Wimberly, and V. Ramakrishnan, *Nature 407*, 340 (2000).
11. C. S. Tung, S. Joseph, and K. Y. Sanbonmatsu, *Nat. Struct. Biol. 9*, 750 (2002).
12. R. Zarivach, E. Ben-Zeev, N. Wu, T. Auerbach, A. Bashan, K. Jakes, K. Dickman, A. Kosmidis, F. Schluenzen, A. Yonath, M. Eisenstein, and M. Shoham, *Biochimie 84* (2002).
13. E. Katchalski-Katzir, I. Shariv, M. Eisenstein, A. A. Friesem, C. Aflalo, and I. A. Vakser, *Proc. Natl. Acad. Sci. USA 89*, 2195 (1992).
14. M. Pioletti, F. Schlunzen, J. Harms, R. Zarivach, M. Gluhmann, H. Avila, A. Bashan, H. Bartels, T. Auerbach, C. Jacobi, T. Hartsch, A. Yonath, and F. Franceschi, *Embo. J. 20*, 1829 (2001).
15. M. Eisenstein, I. Shariv, G. Koren, A. A. Friesem, and E. Katchalski-Katzir, *J. Mol. Biol. 266*, 135 (1997).
16. A. Heifetz, E. Katchalski-Katzir, and M. Eisenstein, *Protein Sci. 11*, 571 (2002).
17. M. Levitt and M. Gerstein, *Proc. Natl. Acad. Sci. USA 95*, 5913 (1998).
18. H. M. Berman, J. Westbrook, Z. Feng, G. Gilliland, T. N. Bhat, H. Weissig, I. N. Shindyalov, and P. E. Bourne, *Nucleic Acids Res 28*, 235 (2000).
19. T. Boon, *Proc. Natl. Acad. Sci. USA 68*, 2421 (1971).
20. C. M. Bowman, J. Sidikaro, and M. Nomura, *Nat. New Biol. 234*, 133 (1971).
21. Y. Kaufmann and A. Zamir, *FEBS Lett. 36*, 277 (1973).
22. Y. Kaufmann and A. Zamir, *Eur. J. Biochem. 53*, 599 (1975).
23. K. Takahashi, and Moore, S., *The Enzymes*. p. 435. Academic Press, New York, 1982.
24. C. Li, D. Zhao, A. Djebli, and M. Shoham, *Structure Fold Des. 7*, 1365 (1999).
25. B. Honig and A. Nicholls, *Science 268*, 1144 (1995).

Date Received: November 13, 2002

Communicated by the Editor
Zippora Shakked